Supplementary Information

Molecular basis of the urate transporter URAT1 inhibition by gout drugs

Yang Suo[1,†], Justin G. Fedor[1,†], Han Zhang[2], Kalina Tsolova[1], Xiaoyu Shi[3], Kedar Sharma[4], Shweta Kumari[2], Mario Borgnia[4], Peng Zhan[3], Wonpil Im[2], Seok-Yong Lee[1*]

Affiliations:

[1]Department of Biochemistry, Duke University School of Medicine, Durham, North Carolina, 27710, USA.

[2]Departments of Biological Sciences, Lehigh University, Bethlehem, Pennsylvania, 18015, USA

[3]Department of Medicinal Chemistry, Key Laboratory of Chemical Biology (Ministry of Education), School of Pharmaceutical Sciences, Cheeloo College of Medicine, Shandong University, Jinan 250012 Shandong, P.R. China

[4] Genome Integrity and Structural Biology Laboratory, National Institute of Environmental Health Sciences, National Institutes of Health, Department of Health and Human Services, Research Triangle Park, NC 27709, USA.

[†] These authors contributed equally.

*Correspondence to:

S.-Y. Lee

Email: seok-yong.lee@duke.edu

Telephone: 919-684-1005

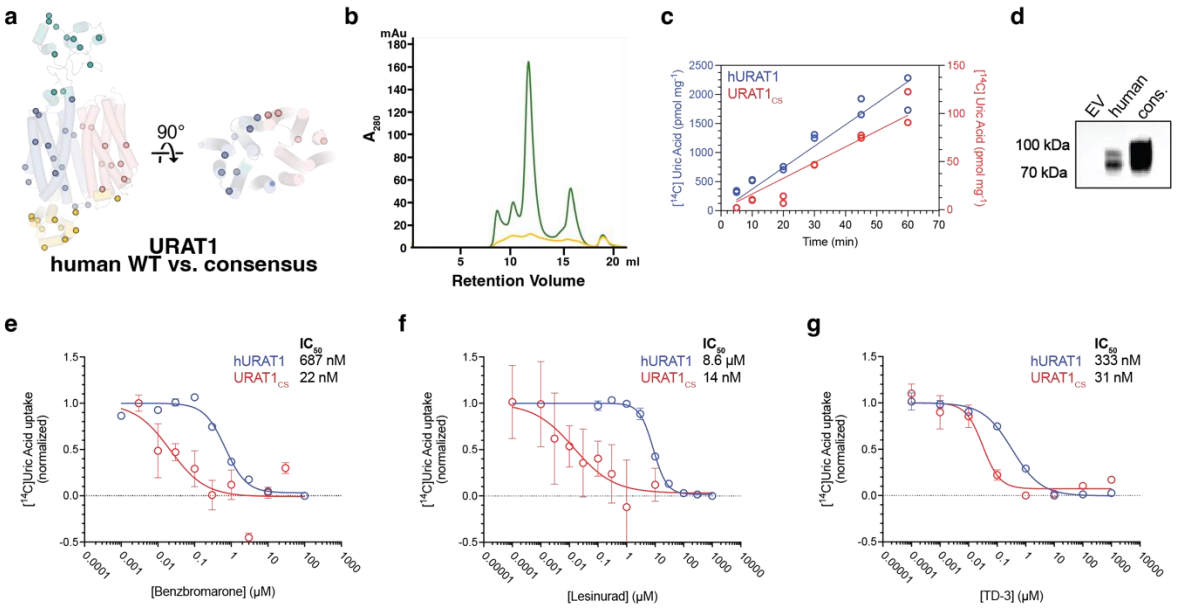

Supplementary Figure 1 | Consensus mutagenesis, functional characterization and protein biochemistry of $URAT1_{CS}$.

a, Mapping of all the mutations of the consensus construct ($URAT1_{CS}$) relative to the hURAT1 sequence. **b**, Gel filtration profiles of purified hURAT1 (yellow) and $URAT1_{CS}$ (green). **c**, Background-corrected uptake of 10 μM [^{14}C]-urate (45 Ci/mol) over time for hURAT1 (left y-axis) and $URAT1_{CS}$ (right y-axis) at 37°C by transiently transfected HEK293T cells, in biological duplicates. **d,** Surface expression western blot from transiently transfected HEK293T cells showing much greater surface expression of $URAT1_{CS}$ relative to hURAT1. **e-g**, IC_{50} determination through background-corrected normalized uptake of 10 μM [^{14}C]-urate (45 Ci/mol) by HEK293T cells transiently expressing hURAT1 (10 min at 37°C) or $URAT1_{CS}$ (30 or 60 min at 37°C) for benzbromarone (**e**), lesinurad (**f**) and TD-3 (**g**). The best-fit IC_{50} values are given and data are represented as means ± SEM, n = 3 biological replicates.

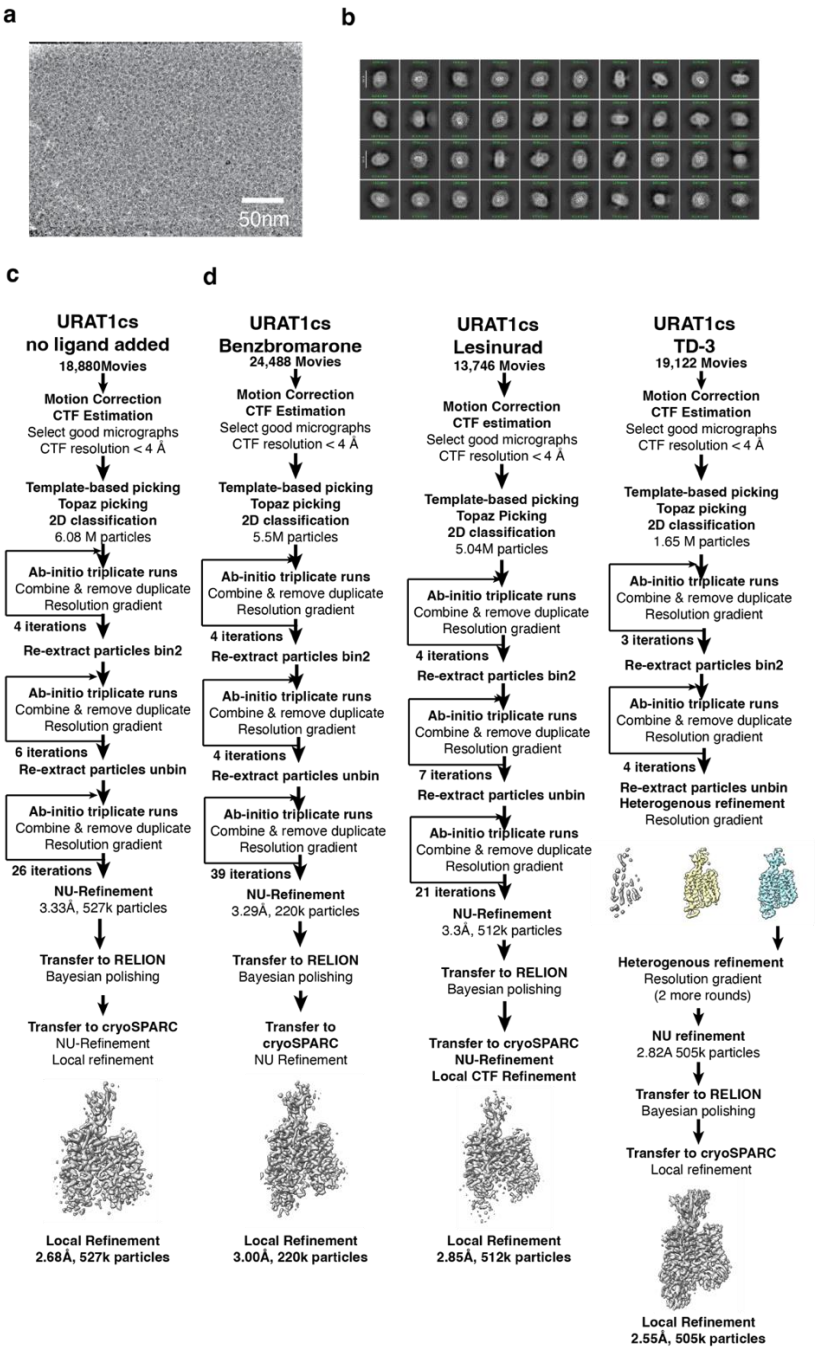

38

39 **Supplementary Figure 2 | Cryo-EM data processing workflow.**

40 Data processing workflow for no ligand added URAT1cs, BBR-URAT1cs, LESU-URAT1cs, and
41 TD-3-URAT1cs datasets, respectively.

42

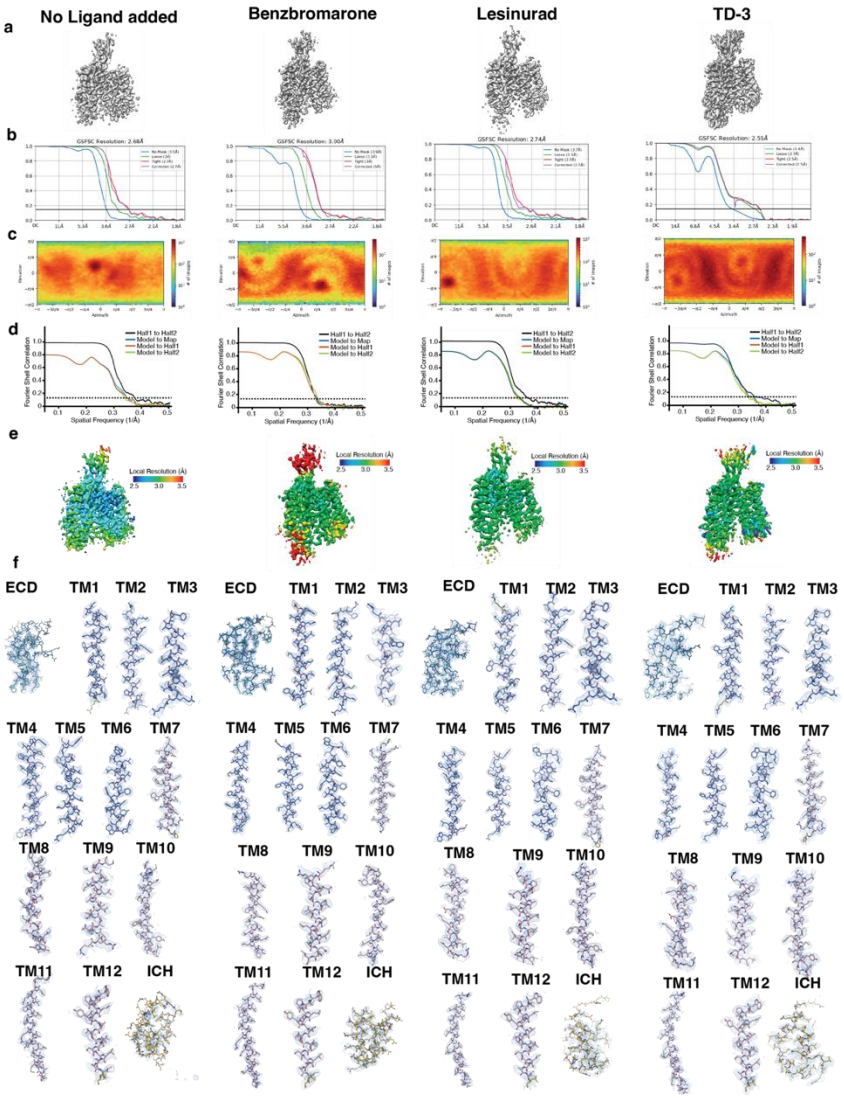

Supplementary Figure 3 | Cryo-EM data validation.

a, Final cryo-EM reconstructions. **b,** Fourier-shell correlation for the final reconstruction, generated from cryoSPARC. **c,** projection orientation distribution map for the final reconstruction, generated from cryoSPARC. **d,** Map-to-model correlation plots. **e,** Local Resolution plots. **f,** cryo-EM maps for secondary structure segments. From left to right are cryo-EM data validations for URAT1$_{CS}$, BBR-URAT1$_{CS}$, LESU-URAT1$_{CS}$, and TD-3-URAT1$_{CS}$ datasets, respectively.

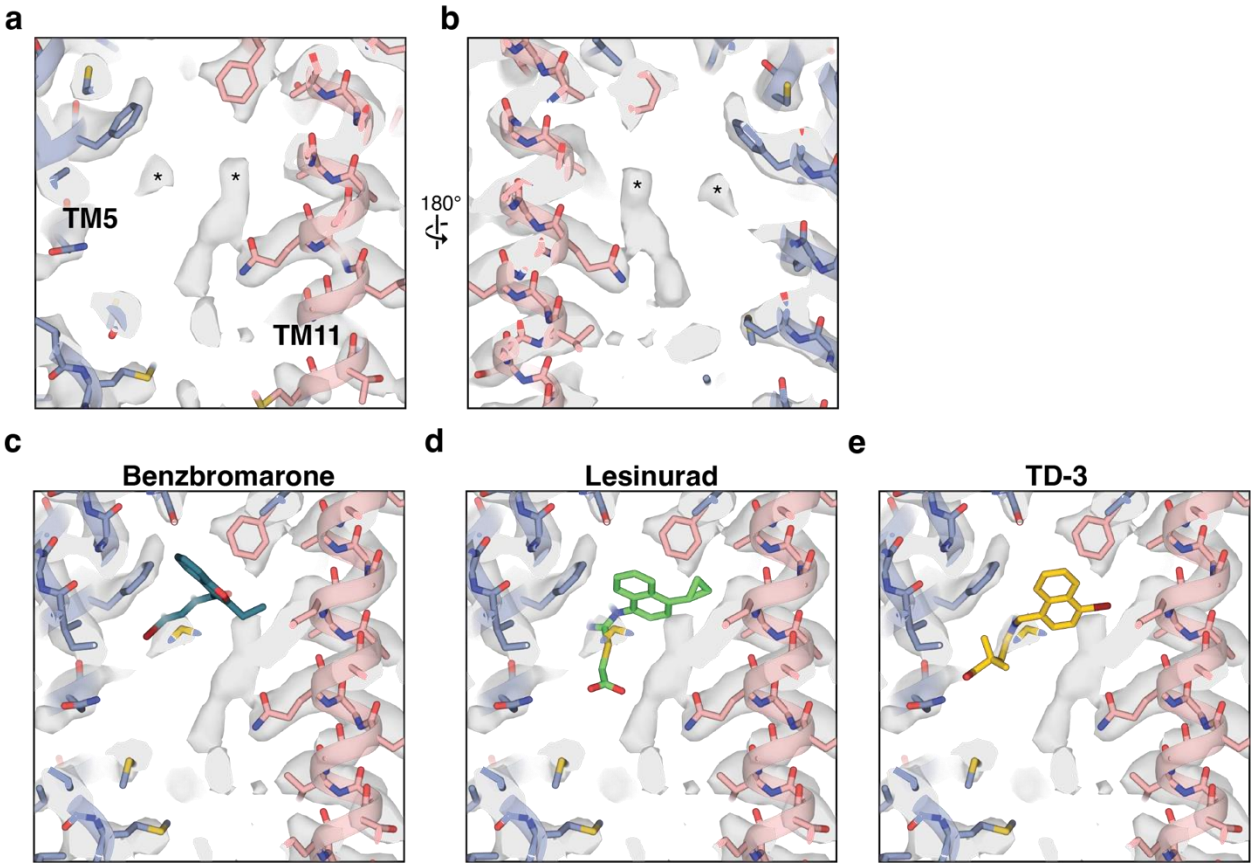

Supplementary Figure 4 | Endogenous cryo-EM peaks in URAT1$_{CS}$ central binding pocket.

a, b, The appearance of unknown cryo-EM peaks in URAT1$_{CS}$ reconstruction without extra ligand added. **c-e,** the map of URAT1$_{CS}$ overlayed with BBR-URAT1$_{CS}$, LESU-URAT1$_{CS}$, or TD-3-URAT1$_{CS}$ coordinates.

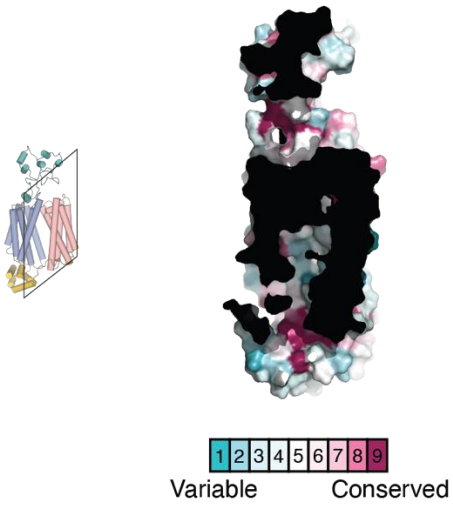

Supplementary Figure 5 | Sequence conservation of URAT1 binding pocket.

Consurf analysis[71] of sequence conservation for URAT1 mapped onto the no inhibitor added structure. The degree of sequence conservation as indicated by the gradient key.

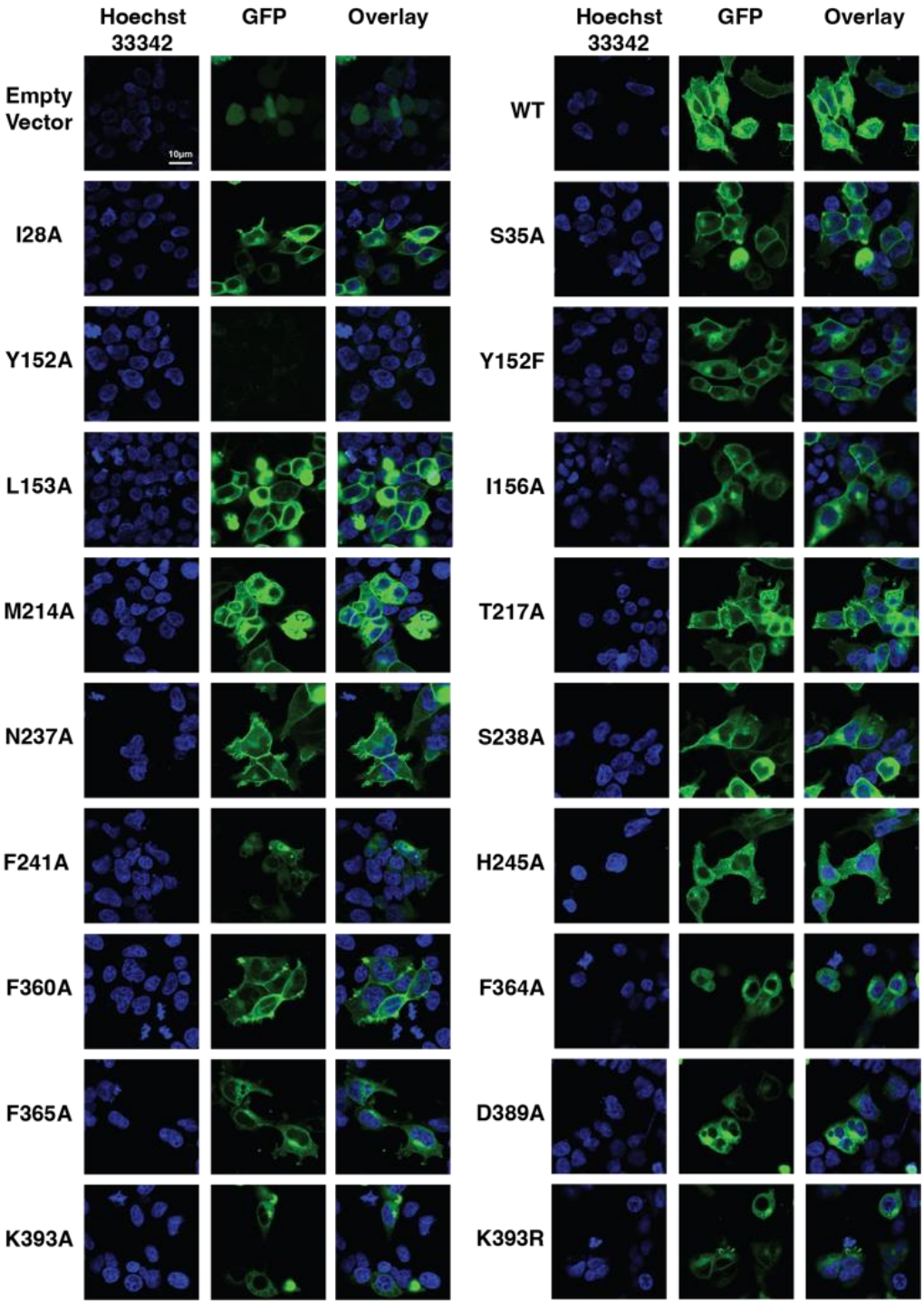

Supplementary Figure 6 | Surface expression of URAT1 and mutants

Microscope images showing bright field, fluorescence and overlay images for the mutants tested in this study. All variants show expression except for Y152A. WT = hURAT1.

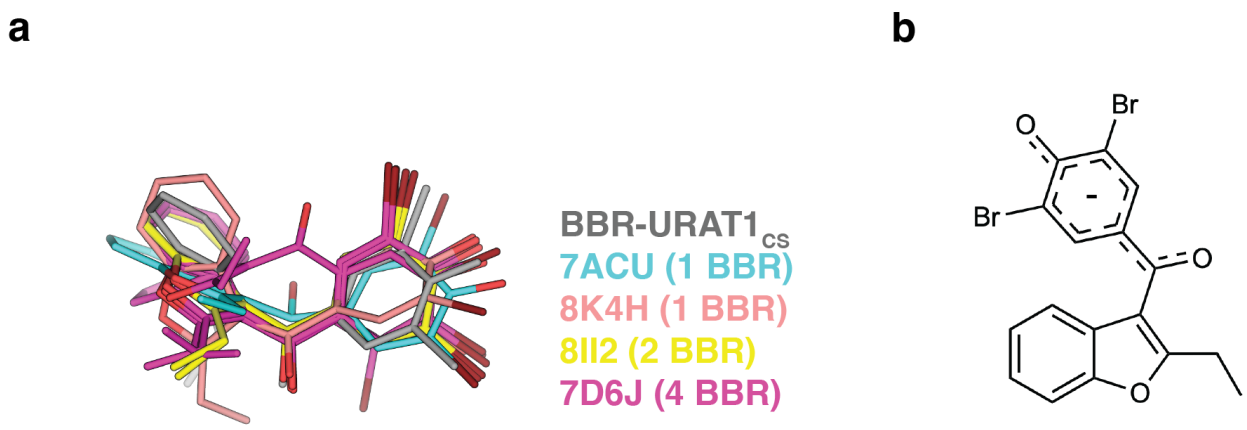

Supplementary Figure 7 | Structural features of BBR.

a, Overlay of BBR molecule in BBR-URAT1$_{CS}$ with BBR molecules in PDB 7ACU (1 molecule), 8K4H (1 molecule), 8II2 (2 molecules) and 7D6J (4 molecules). BBR conformation in BBR-URAT1$_{CS}$ is similar with 6 out of 8 occurrences. **b,** Resonant charge distribution of BBR at physiological pH, adapted from[30].

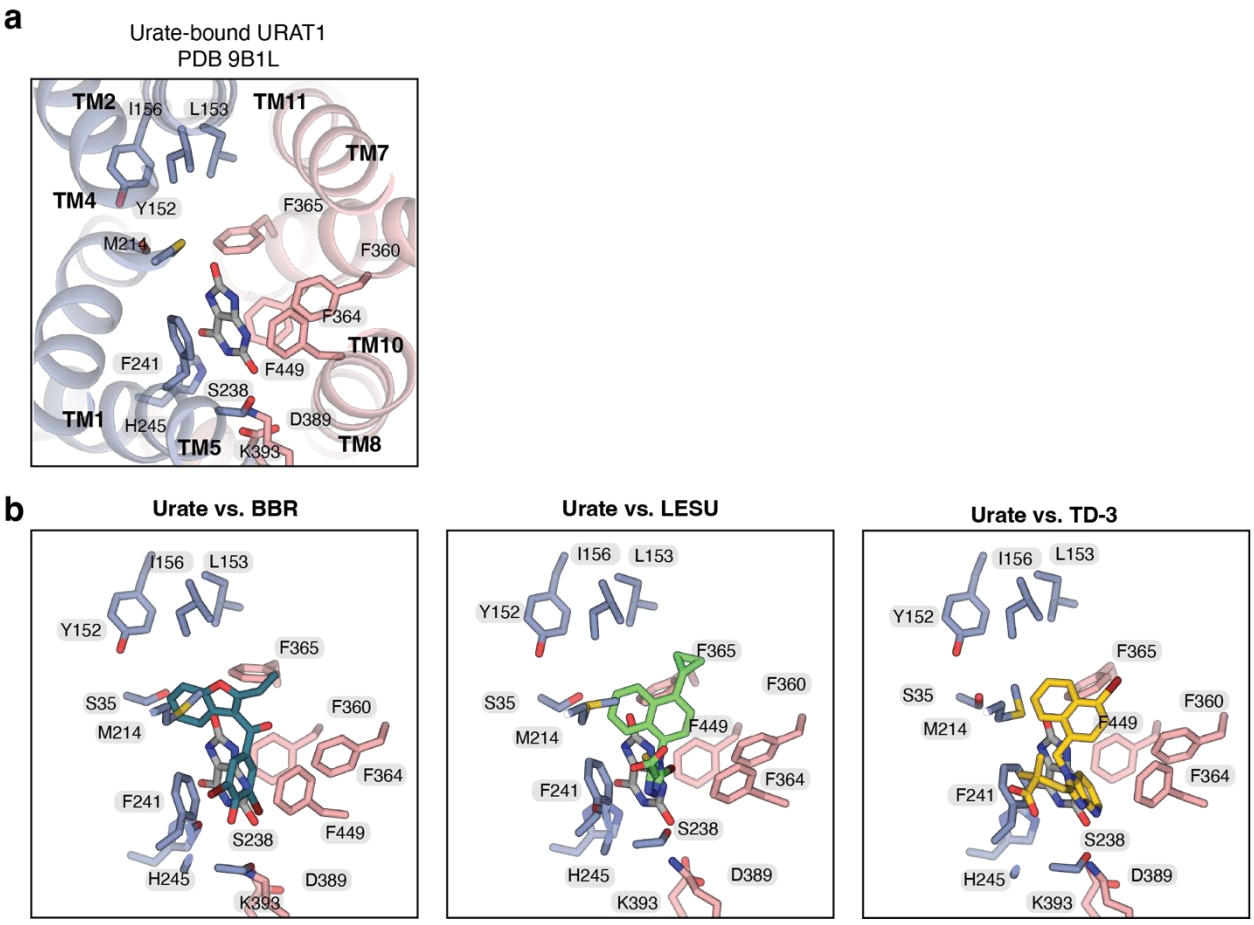

Supplementary Figure 8 | Binding pocket of urate-bound URAT1, adopted from PDB 9B1J[23].

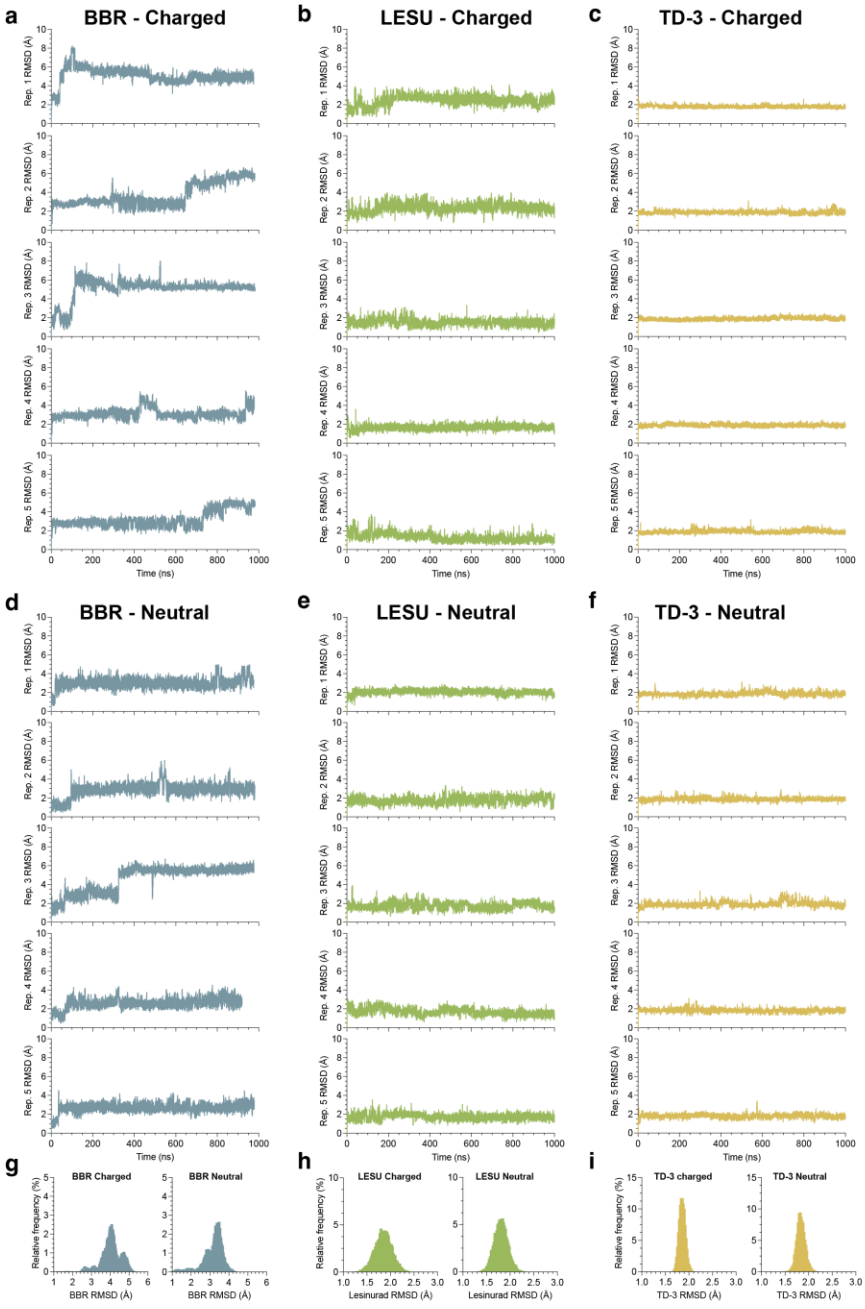

78

79 **Supplementary Figure 9 | Molecular dynamics for URAT1**

80 Replicate sets of 1 μs simulations for either charged (anionic, –1) or neutral forms of BBR (**a,**
81 **d**) , LESU (**b, e**) and TD-3 (**c, f**). g-i, frequency distribution of RMSD values across all five
82 replicates for charged (left) and neutral (right) forms for BBR (**g**), LESU (**h**) and TD-3 (**i**).

83

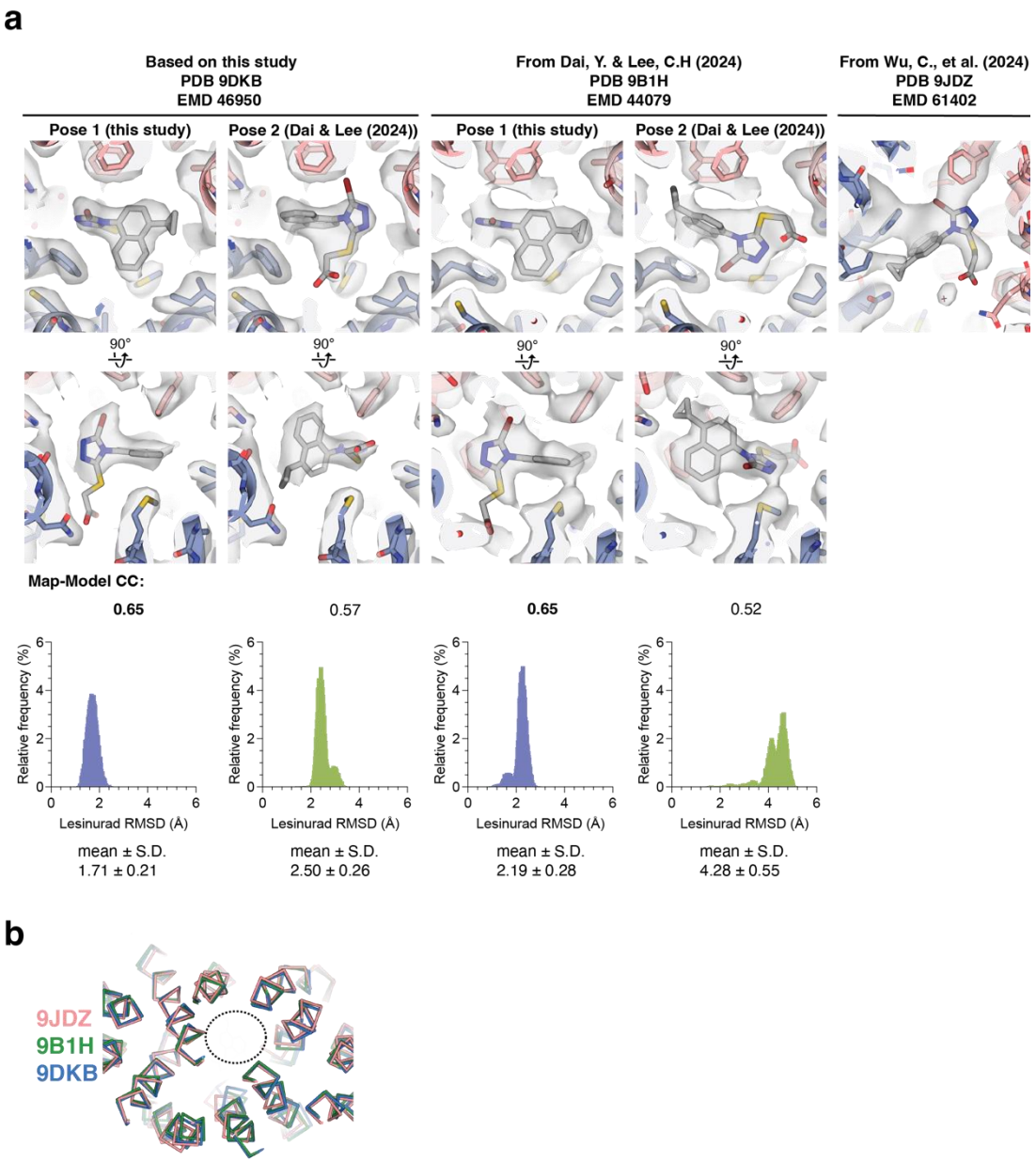

Supplementary Figure 10 | lesinurad model validation and structural comparison

a, Lesinurad binding pose comparison and validation. Lesinurad binding poses from this study (pose 1) compared to that reported by Dai & Lee (pose 2)[23] as modeled into cryo-EM densities from our work and Dai & Lee. The pose from this study not only visually fits better into either map, but also exhibits a higher map-to-model correlation coefficient (Map-Model CC) in either map. MD simulations were conducted of lesinurad in pose 1 or pose 2 in models from this work (PDB 9DKB) or from Dai & Lee (PDB 9B1H). The ligand RMSD values from five replicates of 1 µs simulations each are shown in the histograms, along with distribution mean and standard deviation. The pose 1 (this work) exhibits superior stability when docked into either model, having a lower mean RMSD and narrower spread. The pose and map from Wu, C., *et al.*[31] are also shown for comparison, but its suboptimal cryo-EM density precludes similar analyses. **b**,

Overlay of central binding pocket of lesinurad-bound URAT1 structures of 9JDZ[31] (salmon), 9B1H[23] (green) and 9DKB (this study, marine), showing the similarity of transporter conformation (Cα RMSD ≤ 1Å). Dotted circle indicates central cavity region.

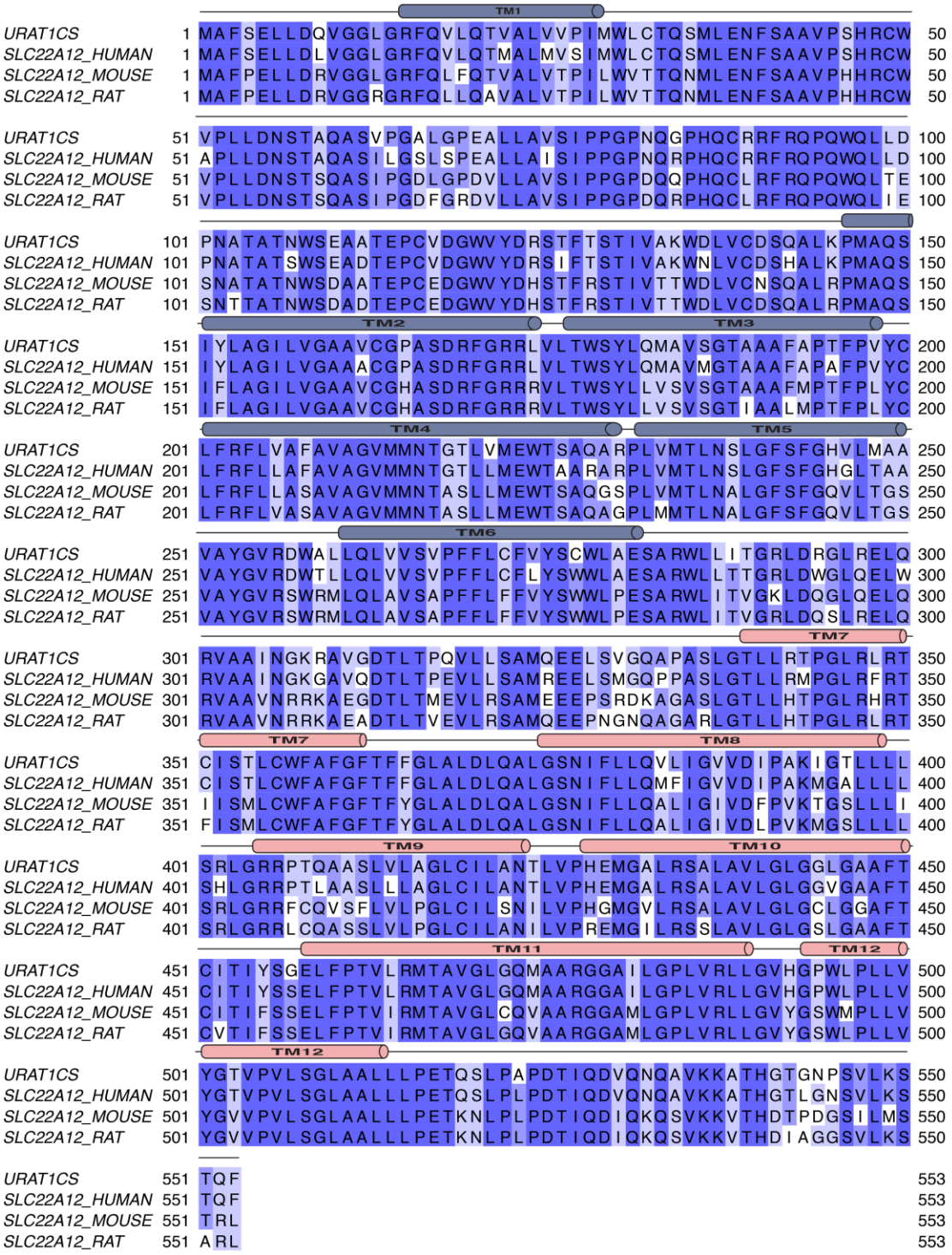

Supplemental Figure 11 | Sequence alignment of URAT1$_{CS}$, human, mouse and rat URAT1 (SLC22A12). Sequence alignment performed using MAFFT[46].

Source data for Supplementary Figure 1d.

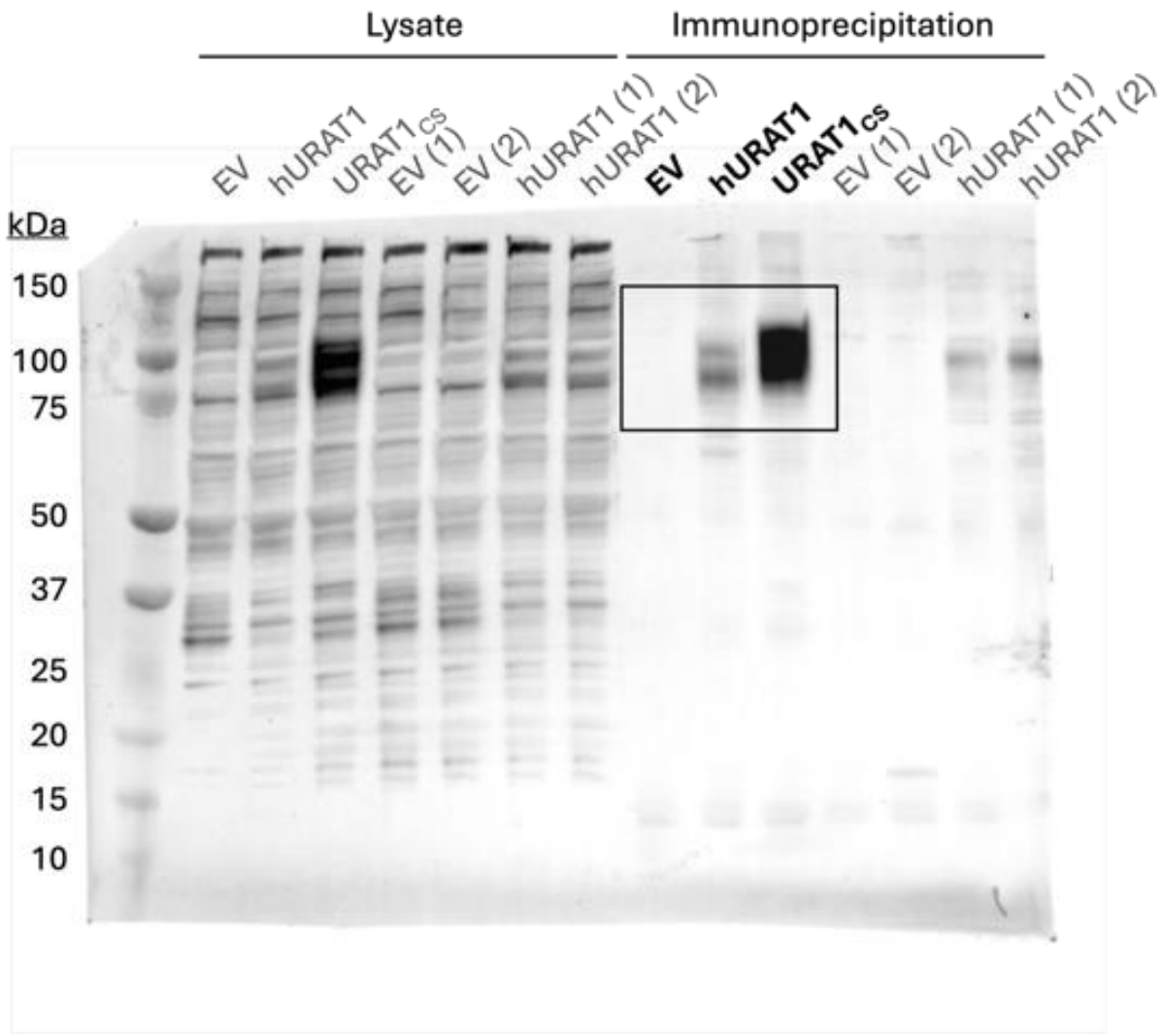

The uncropped blots used in Supplementary Figure 1d. Box indicates cropped region.